

Electronic Structure and Mott Localization in Iron Deficient $\text{TlFe}_{1.5}\text{Se}_2$ with Superstructures

Chao Cao¹ and Jianhui Dai^{1,2}

¹Condensed Matter Physics Group, Department of Physics,
Hangzhou Normal University, Hangzhou 310036, China

²Department of Physics, Zhejiang University, Hangzhou 310027, China

(Dated: November 12, 2018)

Electronic structure and magnetic properties for iron deficient $\text{TlFe}_{2-x}\text{Se}_2$ compounds are studied by first-principles calculations. We find that for the case of $x = 0.5$ with a Fe-vacancy ordered orthorhombic superstructure, the ground state exhibits a stripe-like antiferromagnetic ordering and opens a sizable band gap if the short-ranged Coulomb interaction of Fe-3d electrons is moderately strong, manifesting a possible Mott insulating state. While increasing Fe-vacancies from the $x = 0$ side, where the band structure is similar to that of a heavily electron-doped FeSe system, the Mott localization can be driven by kinetic energy reduction as evidenced by the band narrowing effect. Implications of this scenario in the recent experiments on $\text{TlFe}_{2-x}\text{Se}_2$ are discussed.

PACS numbers: 71.10.Hf, 71.27.+a, 71.55.-i, 75.20.Hr

The discovery of superconductivity (SC) with critical temperatures up to 56 K in iron pnictides [1–6] has triggered renewed interest in searching new route to high-temperature SC. Considerable concerns have been focused on the nature of the parent compounds which show variable bad metal behavior[7] and a universal strip-like antiferromagnetic (SDW) order[8]. The magnetic ordering was proposed to be the consequence of the low energy states (or itinerant electrons) within the nearly nested Fermi surfaces, and hence the Fermi surface nesting is responsible to SC when the SDW order is suppressed [9–11]. An alternative possibility is that the magnetic structure is due to the strong correlation among the Fe-3d electrons, so that the states far away from the Fermi surfaces should be taken into account as well. To this end, Fermi surface nesting is not a necessary ingredient and the J_1 - J_2 Heisenberg model based on the local moment picture could be an appropriate starting point. [12–14, 16]

Most recently, Fang *et al.* [17] reported that the Fe-deficient compounds $(\text{Tl,K})\text{Fe}_{2-x}\text{Se}_2$ exhibit SC with T_c up to ~ 31 K for $x = 0.12 \sim 0.3$. Special interest in this class of materials is that the SC emerges in proximity to an insulating phase. It is yet unknown whether this insulating phase is a Mott insulator driven by Fe-3d electron correlations. Theoretically, this possibility is mysterious, as previous first-principle calculations on both TlFe_2Se_2 [18] and KFe_2Se_2 [19, 20] with the ThCr_2Si_2 structure (122-type) suggest that the parent compounds of the ternary iron chalcogenides should be metallic with either checkerboard antiferromagnetic (AFM) (for Tl-122)[18] or SDW (for K-122)[20] order, much like the electron overdoped 11-type iron selenides. Experimentally, it has been reported recently that the alkali intercalated compounds $\text{K}_{0.8}\text{Fe}_2\text{Se}_2$ [21] and $\text{Cs}_{0.8}\text{Fe}_2\text{Se}_{1.96}$ [22] (both iso-structural to BaFe_2As_2), while superconducting under 30 K and 27 K respectively, exhibit the metallic behavior in their normal states.

Two closely related questions thus arise: What is the ground state of the "parent" compound of these superconducting ternary iron chalcogenides of 122-type structure, and how can a Mott-insulating phase develop and then diminish with in-

creasing Fe-content or *electron doping* giving way to SC?

In this paper, we suggest partial answers to the questions by first-principles study on $\text{TlFe}_{2-x}\text{Se}_2$. We start from and pay special attention to the case with $x = 0.5$, which is stoichiometrically equivalent to $\text{Tl}_2\text{Fe}_3\text{Se}_4$ but with the 122-type structure. Hence, Fe^{2+} is the nominal valence as in other iron pnictides/chalcogenides. Our calculation shows that the ground state of $\text{TlFe}_{1.5}\text{Se}_2$ with Fe-vacancy ordered orthorhombic superstructure is an SDW phase which can open a sizable gap if a moderately strong electron correlation is imposed. The quantitative change of the bandwidth of Fe-3d electrons further supports the Mott localization driven by kinetic energy reduction due to Fe-vacancies. This scenario is quite similar to the Mott localization proposed for iron oxychalcogenides $\text{La}_2\text{O}_2\text{Fe}_2\text{O}(\text{Se,S})_2$ [23], where the reduction of kinetic energy or the band narrowing is due to the expanded interatomic Fe-Fe distance. We will discuss the implications of this scenario in the recent experiments on $\text{TlFe}_{2-x}\text{Se}_2$.

The electronic structure calculations were performed with the Vienna Ab-initio Simulation Package (VASP)[24, 25]. All structures were optimized so that the forces on individual atoms were smaller than 0.02 eV/\AA and the pressure convergence criterion is chosen to be 0.5 kbar. For the optimization and ground state calculations, a $8 \times 4 \times 4$ Monkhorst-Pack k-grid[26] was employed, while $16 \times 8 \times 8$ Monkhorst-Pack k-grid was used for the density of states (DOS) calculations. The PBE flavor of general gradient approximation (GGA) to the exchange-correlation functional[27] was applied throughout the calculations.

We first discuss the possible crystal structure and spin configurations of $\text{TlFe}_{1.5}\text{Se}_2$. The Mössbauer experiment suggests a body-centered orthorhombic (BCO) crystal structure [28], where the Fe sheets form superstructure due to Fe-deficiency (FIG. 1). There are four possible stacking configurations for the two neighbouring Fe-layers[32], as shown in FIG. 1. We consider the AFM and SDW configurations within each layers, while the interlayer coupling along c-axis can be either ferromagnetic (FM) or AFM. The relative energies for

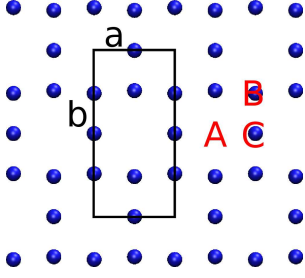


FIG. 1: Superstructure of $\text{TlFe}_{1.5}\text{Se}_2$. A , B , and C correspond to three different sites directly above the Fe-vacancy, the 3-coordinated Fe site, and the 2-coordinated site, respectively. Another stacking pattern A' is that the upper-layer is rotated 90° around c -axis.

different stacking and ordering patterns are listed in Table I. We find that the ground state (for $x = 0.5$) should be of essentially two-dimensional SDW, as the energy differences among the different inter-layer magnetic orderings are very small ($< 5\text{meV/Fe}$), indicating the negligible inter-layer magnetic coupling at this state. Hence, without losing generality, we shall focus on the AA -stacking pattern in the following discussions.

We also notice that for the NM state, the full structural optimization leads to the well-known c -collapse problem; while for the SDW state, the resulting structure (c and z_{Se}) is within the expectation. Thus, unless otherwise specified, the electronic structure calculations in the following discussions were performed with the geometry relaxed in the SDW configuration. The calculated local magnetic moment of Fe atom is then $m_{\text{Fe}} \approx 2.6 \sim 2.7 \mu_B$.

TABLE I: Configuration energies of $\text{TlFe}_{1.5}\text{Se}_2$ (in unit of meV). AA , AB , AC and AA' indicates the stacking geometry, while NM, AFM, SDW indicate the intralayer magnetic configurations. The superscripts a and f indicate interlayer AFM and FM orderings.

	AA	AB	AC	AA'
NM	0.0	9	3	12.7
AFM ^f	-200	-177	-172	
AFM ^a	-173	-177	-174	
SDW ^f	-268	-268	-270	
SDW ^a	-273	-268	-269	

We now examine the DOS of the AA -stacking SDW^a plotted in Fig. 2(a), which exhibits a sharp dip around the Fermi energy. We find that the band gap E_g is vanishingly small for the fully optimized system under the GGA method. Furthermore, the AB - and AC -stacking SDW^a states, which are almost degenerate to the AA -stacking SDW^a, are both metallic, with 0.216 states/(eV·Formula) and 0.656 states/(eV·Formula) respectively. Hence, the three stacking patterns may coexist at low temperatures. The SDW band gap, if exists, is too small to compare with the activation gap $E_a \sim 57.7$ meV observed in the $x = 0.5$ sample [17]. It indicates that the observed activation gap in $\text{TlFe}_{2-x}\text{Se}_2$ (at least for $x = 0.5$) is not due to the SDW ordering itself.

TABLE II: Geometry and magnetic properties of $\text{TlFe}_{1.5}\text{Se}_2$. Only the ground state (SDW^a) configurations are listed. z_{Se} is the internal coordinate for Se and m_{Fe} is the local magnetic moment on Fe atoms. The numbers outside and inside the brackets for m_{Fe} are for 3-coordinated and 2-coordinated Fe atoms, respectively.

		AA	AB	AC
SDW ^a	a	5.4824	5.5407	5.5483
	b	11.0519	11.0497	11.0270
	c	13.8162	13.7892	13.8176
	z_{Se}	0.351	0.351(0.350)	0.350
	$m_{\text{Fe}}(\mu_B)$	2.60(2.73)	2.61(2.74)	2.62(2.74)

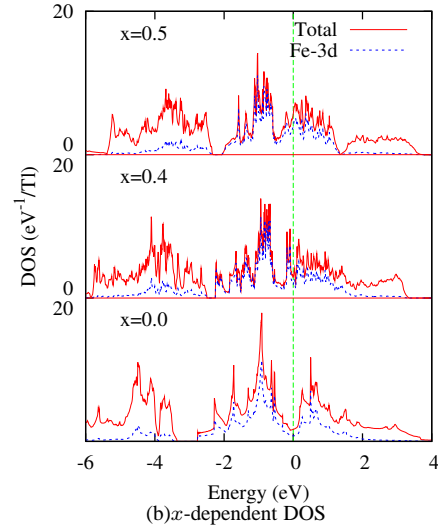
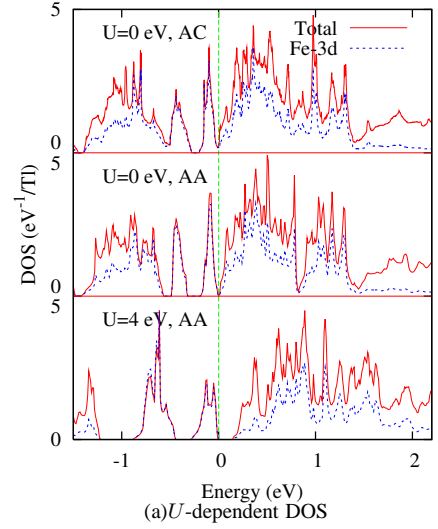


FIG. 2: Total and projected density of states of $\text{TlFe}_{2-x}\text{Se}_2$. 2(a): The U -dependent DOS at the SDW state for $x = 0.5$; 2(b): The x -dependent DOS at the NM state for $U = 0$ with Fe-vacancy superstructures. In 2(a), only α -spin DOS is shown since both spin are degenerate. All plots are renormalized to per $\text{TlFe}_{2-x}\text{Se}_2$ formula.

Here, we suggest that the sizable activation gap can be attributed to the Mott localization driven by the moderately strong electron correlation. To seek for this possibility, we extended our calculations by using the GGA+ U method. The calculated DOS for $U = 0$ eV and $U = 4.0$ eV are compared in FIG. 2(a). Within GGA+ U , an insulating gap develops immediately with increasing U , which turns out to be 40, 60, 80, 140, and 230 meV for $U=1,2,3,4$, and 5 eV, respectively. The projected DOS associated with Fe-3d electrons move to higher energies mainly distributed around 1 eV above the Fermi energy (for $U=4$ eV).

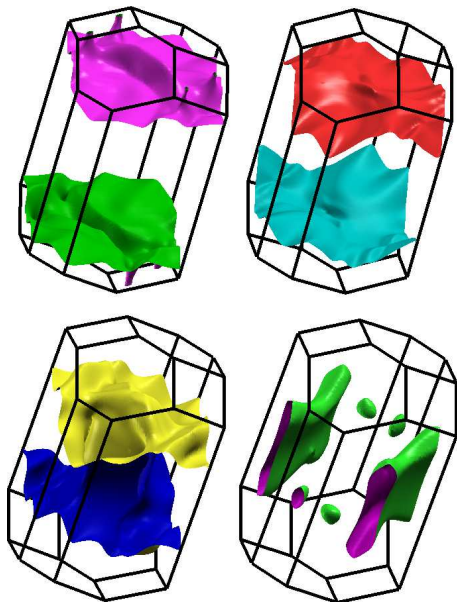


FIG. 3: The Fermi surfaces (for $x = 0.5$ and $U = 0$) reconstructed using the MLWFs shown in the Γ -centered reciprocal BCC lattice.

We also performed calculations for $x = 0, 0.4$, keeping the Fe-vacancy ordered tetragonal superstructure in the latter case [17, 28]. For $x = 0$ the AFM state becomes more stable than the SDW state (in agreement with Ref.[18]), while the overall band structure and Fermi surface (FS) of TlFe_2As_2 are similar to that of KFe_2Se_2 [20]. For illustration, the band structures for $x = 0, 0.5$ in the NM states are fitted to a tight-binding model Hamiltonian by using the maximally localized wannier function (MLWF)[29, 30] method. The results are plotted in Fig. 4, where the color indicates the percentage of $d_{zx(y)}$ and $d_{y^2-x^2}$ composition, from 0% (blue) to 100% (red). For $x = 0$, the Hamiltonian is particularly simple with 5-bands. The nearest neighbor hopping parameters and the on-site energies are listed in TAB. IV. The bands near E_F are dominated by $d_{zx(y)}$ and $d_{y^2-x^2}$ orbitals except for one empty band around X. For $x = 0.5$, the Hamiltonian is too complicated due to the structural distortion, and all 5 d-orbitals are entangled considerably around E_F . Nevertheless, the FS of $\text{TlFe}_{1.5}\text{Se}_2$ can be reconstructed as shown in Fig. 3.

The apparent different band structures for $x = 0$ and 0.5, together with the drastic change in their FS topologies, pro-

vide an indication for the transition at certain $0 < x_c < 0.5$, i.e., when $x > x_c$, the Mott localization takes place. As the Fe-Fe distance increases less than 1% from $x = 0$ to $x = 0.5$ [17], this amount of lattice expansion is not sufficient for the Mott localization in $\text{TlFe}_{2-x}\text{Se}_2$, as compared to iron oxychalcogenides $\text{La}_2\text{O}_2\text{Fe}_2\text{O}(\text{Se,S})_2$ [23]. Here, we argue that the kinetic energy reduction caused by the Fe-vacancies should play an crucial role in driving the system to the insulating phase. An intuitive estimate is that the coordinate number of Fe in the $\text{TlFe}_{1.5}\text{Se}_2$ is reduced to 3 or 2 depending on the Fe site comparing to 4 in a perfect square lattice. Thus the total kinetic energy is substantially reduced by the Fe-vacancies, enhancing the normalized electron correlation U/W , with W being the bandwidth proportional to the kinetic energy.

Our argument can be checked by fitting band structures of $x = 0, 0.4$ and 0.5 to the tight-binding models. We only need to consider the NM state (and $U = 0$) and calculate the sum of the nearest neighbor hoppings (absolute values) among all five d-orbitals around a specific Fe atom. It serves as an approximate upper limit of the total kinetic energy E_K . Using the fitted hopping parameters we obtain $E_K = 15.59$ and 9.98 eV for $x = 0$ and 0.4, respectively. While for $x = 0.5$, we obtain $E_K = 11.34$ or 6.87 eV, corresponding to 3- or 2-coordinated Fe-sites, respectively. As the ratio of their numbers is 2:1, the average kinetic energy is 9.85 eV. For comparison, the DOS at the NM state when $U = 0$ for $x = 0, 0.4$, and 0.5 are plotted in Fig. 2(b). The Fe-3d bandwidths are roughly 4.8 eV, 3.8 eV, and 3.5 eV, respectively. Thus, we indeed find a substantial enhancement of the normalized electron correlation, manifesting the kinetic energy reduction caused by Fe-vacancies.

TABLE III: Pressure dependency of crystal structure and band gap for $x = 0.5$ and $U = 4.0$ eV.

P (GPa)	0	2	4	6
a (\AA)	5.5507	5.4517	5.3716	5.3079
b (\AA)	11.0342	10.8842	10.7283	10.6177
c (\AA)	13.8027	13.5166	13.2874	13.1102
E_{cell} (eV)	-187.01	-186.65	-185.91	-158.00
E_g (meV)	140	80	50	0

Finally, we remark that our calculations assume homogeneous formation of the Fe-vacancy ordered superstructures. If this is the case in real materials, the activation gap observed in the $x = 0.5$ sample should be not due to the Anderson localization caused by vacancy disorder effect. As the Mott (de-)localization is sensitive to physical pressure which can lead to monotonous bandwidth expansion by lattice contraction, we expect that the gap dependence on pressure can be used to test this scenario. The numerical results for the pressure dependent band gap E_g with fixed $U = 4.0$ eV are listed in TAB. III ($x = 0.5$). From these results we expect that the activation gap, which is about 60 meV or well below 150 meV [17] under ambient pressure, can be completely suppressed by applying pressure up to ~ 6 GPa and then the SC may emerge.

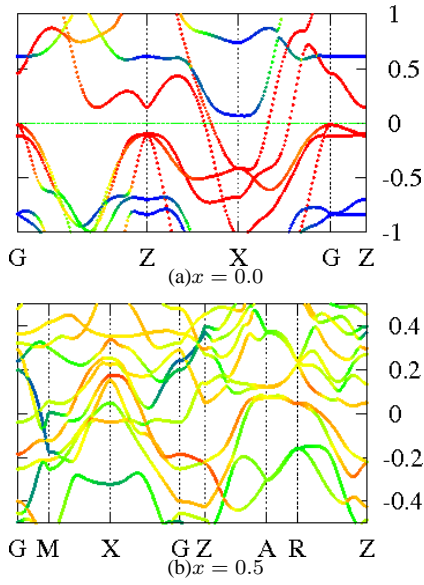


FIG. 4: Band structures of $\text{TlFe}_{2-x}\text{Se}_2$ fitted using MLWF.

TABLE IV: Tight-binding Hamiltonian for TlFe_2Se_2 . Only the nearest neighbor hoppings and on-site energies (diagonal line in the brackets) are shown here. All numbers are in eV.

	d_{z^2}	d_{zx}	d_{zy}	$d_{x^2-y^2}$	d_{xy}
d_{z^2}	-0.019 (4.765)	0	0.156	0.303	0
d_{zx}	0	-0.028 (5.084)	0	0	0.286
d_{zy}	0.156	0	-0.314 (5.084)	-0.344	0
$d_{x^2-y^2}$	-0.303	0	-0.344	-0.378 (4.600)	0.0
d_{xy}	0	0.286	0	0	-0.047 (5.056)

To summarize, we find that for $\text{TlFe}_{1.5}\text{Se}_2$, the electronic band structure shows a sizable band gap if the short-ranged Coulomb interaction U beyond LDA/GGA is considered. From the experimentally observed activation gap, U should be at least 2eV. The corresponding ground state is then a stripe-like anti-ferromagnetic Mott insulator. The superstructure of various Fe-vacancy ordering patterns is important for the stability of the Mott insulating phase and kinetic energy reduction caused by the vacancies plays a crucial role for the Mott localization. The pressure dependence of the gap behavior could be used to test this possibility.

We would like to express special thanks to M. Fang and Q. Si for helpful discussions. We are also grateful for the discussions with G. Cao, H. Wang, Z. Xu, H. Yuan. This work was supported by the NSFC, the 973 Project of the MOST and the Fundamental Research Funds for the Central Universities of China (No. 2010QNA3026). All the calculations were per-

formed at High Performance Computing Center of Hangzhou Normal University.

Note added: After completing this work, we became aware of two recent papers by X.W. Yan et al.[31], where independent first-principles studies on the cases of $x = 0$ and $x = 0.5$ were reported.

-
- [1] Y. Kamihara, T. Watanabe, M. Hirano, and H. Hosono, *J. Am. Chem. Soc.* **130**, 3296 (2008).
 - [2] X. H. Chen, G. W. T. Wu, R. H. Liu, H. Chen, and D. F. Fang, *Nature* **453**, 761 (2008).
 - [3] G. F. Chen, Z. Li, D. Wu, G. Li, W. Z. Hu, J. Dong, P. Zheng, J. L. Luo, and N. L. Wang, *Phys. Rev. Lett.* **100**, 247002 (2008).
 - [4] Z. Ren, G. Che, X. Dong, J. Yang, W. Lu, W. Yi, X. Shen, Z. Li, L. Sun, F. Zhou, et al., *Europhys. Lett.* **83**, 17002 (2008).
 - [5] H. H. Wen, G. Mu, L. Fang, H. Yang, and X. Zhu, *Europhys. Lett.* **82**, 17009 (2008).
 - [6] C. Wang, L. Li, S. Chi, Z. Zhu, Z. Ren, Y. Li, Y. Wang, X. Lin, Y. Luo, X. Xu, et al., *Europhys. Lett.* **83**, 67006 (2008).
 - [7] M. M. Q. *et al.*, *Nature Phys.* **5**, 647 (2009).
 - [8] C. de la Cruz *et al.*, *Nature* (453).
 - [9] J. D. *et al.*, *Europhys. Lett.* **83**, 270069 (2008).
 - [10] D. J. Singh and M. H. Du, *Phys. Rev. Lett.* **100**, 237003 (2008).
 - [11] I. I. Mazin, D. J. Singh, M. D. Johannes, and M. H. Du, *Phys. Rev. Lett.* **101**, 057003 (2008).
 - [12] T. Yildirim, *Phys. Rev. Lett.* **101**, 057010 (2008).
 - [13] Q. Si and E. Abrahams, *Phys. Rev. Lett.* **101**, 076401 (2008).
 - [14] C. Cao, P. J. Hirschfeld, and H.-P. Cheng, *Phys. Rev. B* **77**, 220506 (2008).
 - [15] F. Ma and Z. Y. Lu, *Phys. Rev. B* **78**, 033111 (2008).
 - [16] F. Ma, Z. Y. Lu, and T. Xiang, *Phys. Rev. B* **78**, 2245179 (2008).
 - [17] M. Fang, H. Wang, C. Dong, Z. Li, Li, C. Feng, J. Chen, and H. Yuan (2010), arXiv:1012.5236.
 - [18] L. Zhang and D. J. Singh, *Phys. Rev. B* **79**, 094528 (2009).
 - [19] I. Shein and A. Ivanovskii (2010), arXiv:1012.5164.
 - [20] C. Cao and J. Dai (2010), arXiv:1012.5621.
 - [21] J. Guo, S. Jin, G. Wang, K. Zhu, M. He, and X. L. Chen, *Phys. Rev. B* **82**, 180520(R) (2010).
 - [22] A. K.-M. *et al.* (2010), arXiv:1012.3637.
 - [23] J. X. Zhu, R. Yu, H. Wang, L. L. Zhao, M. D. Jones, J. Dai, E. Abrahams, E. Morosan, M. H. Fang, and Q. Si, *Phys. Rev. Lett.* **104**, 216405 (2010).
 - [24] G. Kresse and J. Hafner, *Phys. Rev. B* **47**, 558 (1993).
 - [25] G. Kresse and D. Joubert, *Phys. Rev. B* **59**, 1758 (1999).
 - [26] H. J. Monkhorst and J. D. Pack, *Phys. Rev. B* **13**, 5188 (1976).
 - [27] J. Perdew, K. Burke, and M. Ernzerhof, *Phys. Rev. Lett.* **77**, 3865 (1996).
 - [28] L. Haggstrom and A. Seidel, *J. Mag. Mat.* **98**, 37 (1991).
 - [29] I. Souza, N. Marzari, and D. Vanderbilt, *Phys. Rev. B* **65**, 035109 (2001).
 - [30] A. A. Mostofi, J. R. Yates, Y.-S. Lee, I. Souza, D. Vanderbilt, and N. Marzari, *Comp. Phys. Comm.* (2007), arXiv:0708.0650.
 - [31] X. W. Yan, M. Gao, Z. Y. Lu, and T. Xiang (2010), arXiv:1012.5536v1; arXiv:1012.6015v1.
 - [32] We find that the Fe-deficiency will induce structural relaxation in general, which leads to the distortion of the square Fe lattice and the small displacement of Fe atoms. Thus the AA' -stacking is energetically unfavorable and is not considered here.